



HAL
open science

A molecular framework for the control of adventitious rooting by TIR1/AFB2-Aux/IAA-dependent auxin signaling in Arabidopsis

Abdellah Lakehal, Salma Chaabouni, Emilie Cavel, Rozenn Le Hir, Alok Ranjan, Zahra Raneshan, Ondrej Novák, Daniel Pacurar, Irene Perrone, François Jobert, et al.

► To cite this version:

Abdellah Lakehal, Salma Chaabouni, Emilie Cavel, Rozenn Le Hir, Alok Ranjan, et al.. A molecular framework for the control of adventitious rooting by TIR1/AFB2-Aux/IAA-dependent auxin signaling in Arabidopsis. *Molecular Plant*, 2019, 12 (11), pp.1499-1514. 10.1016/j.molp.2019.09.001 . hal-02621817

HAL Id: hal-02621817

<https://hal.inrae.fr/hal-02621817v1>

Submitted on 20 Jul 2022

HAL is a multi-disciplinary open access archive for the deposit and dissemination of scientific research documents, whether they are published or not. The documents may come from teaching and research institutions in France or abroad, or from public or private research centers.

L'archive ouverte pluridisciplinaire **HAL**, est destinée au dépôt et à la diffusion de documents scientifiques de niveau recherche, publiés ou non, émanant des établissements d'enseignement et de recherche français ou étrangers, des laboratoires publics ou privés.



Distributed under a Creative Commons Attribution - NonCommercial 4.0 International License

1 **A Molecular Framework for the Control of Adventitious Rooting by the TIR1/AFB2-**
2 **Aux/IAA-Dependent Auxin Signaling in Arabidopsis**

3
4 Abdellah Lakehal^{1#}, Salma Chaabouni^{1#}, Emilie Cavel^{1,a}, Rozenn Le Hir², Alok Ranjan¹,
5 Zahra Raneshan^{1,3}, Ondřej Novák^{4,5}, Daniel I. Păcurar¹, Irene Perrone^{1,b}, François Jobert^{6,c},
6 Laurent Gutierrez⁶, Laszlo Bakò¹ and Catherine Bellini^{1,2*}

7
8 ¹ Umeå Plant Science Centre, Department of Plant Physiology, Umeå University, SE-90736
9 Umeå, Sweden

10 ² Institut Jean-Pierre Bourgin, INRA, AgroParisTech, CNRS, Université Paris-Saclay, 78000
11 Versailles, France

12 ³ Department of Biology, Faculty of Science, Shahid Bahonar University, Kerman, Iran

13 ⁴ Laboratory of Growth Regulators, Faculty of Science, Palacký University and Institute of
14 Experimental Botany, The Czech Academy of Sciences, 78371 Olomouc, Czech Republic

15 ⁵ Umeå Plant Science Centre, Department of Forest Genetics and Physiology, Swedish
16 Agriculture University, SE-90183 Umea, Sweden

17 ⁶ Centre de Ressources Régionales en Biologie Moléculaire (CRRBM), Université de Picardie
18 Jules Verne, 80039 Amiens, France

19
20 # These two authors equally contributed to the work.

21 ^a Present address: Centre de Ressources Régionales en Biologie Moléculaire (CRRBM),
22 Université de Picardie Jules Verne, 80039 Amiens, France

23 ^b Present address: Institute for Sustainable Plant Protection, National Research Council of
24 Italy, Turin, Italy

25 ^c Present address: Umeå Plant Science Centre, Department of Forest Genetics and Plant
26 Physiology, SLU, SE-90736 Umeå, Sweden

27
28 * To whom correspondence should be addressed:

29 Pr Catherine Bellini (Catherine.Bellini@umu.se /Catherine.Bellini@inra.fr)
30 Umeå Plant Science Centre, Department of Plant Physiology,

31 Umeå University, SE-90736 Umeå, Sweden

32 Phone: +46907869624

33

34 **Short title:** TIR1/AFBs, AuxIAAs and adventitious rooting

35 **SHORT SUMMARY**

36 Auxin mediates plethora of developmental programs. We provide evidence on how the
37 canonical auxin-sensing machinery functions to control the JA pool during adventitious
38 rooting. We show that TIR1, besides its function in negatively regulating JA biosynthesis,
39 acts with AFB2 and IAA6, IAA9 and IAA17 to form a sensing module regulating the
40 expression of the JA conjugating enzymes GH3.3, GH3.5 and GH3.6.

41

42 **ABSTRACT**

43 In *Arabidopsis thaliana*, canonical auxin-dependent gene regulation is mediated by 23
44 transcription factors from the AUXIN RESPONSE FACTOR (ARF) family interacting with
45 29 auxin/indole acetic acid repressors (Aux/IAA), themselves forming coreceptor complexes
46 with one of six TRANSPORT INHIBITOR1/AUXIN-SIGNALING F-BOX (TIR1/AFB)
47 PROTEINS. Different combinations of co-receptors drive specific sensing outputs, allowing
48 auxin to control a myriad of processes. Considerable efforts have been made to discern the
49 specificity of auxin action. However, owing to a lack of obvious phenotype in single loss-of-
50 function mutants in *Aux/IAA* genes, most genetic studies have relied on gain-of-function
51 mutants, which are highly pleiotropic. *ARF6* and *ARF8* are positive regulators of adventitious
52 root initiation upstream of jasmonate, but the exact auxin co-receptor complexes controlling
53 the transcriptional activity of these proteins was still unknown. Here using loss-of-function
54 mutants we show that *IAA6*, *IAA9* and *IAA17* genes act additively in the control of AR
55 initiation, and by performing protein-protein interaction analysis, we show that the
56 corresponding proteins interact with ARF6 and/or ARF8 and likely repress their activity. We
57 also demonstrate that *TIR1* and *AFB2* are positive regulators of adventitious root formation
58 and suggest a dual role for TIR1 in the control of JA biosynthesis and conjugation, as
59 revealed by upregulation of several JA biosynthesis genes in the *tir1-1* mutant. We propose
60 that in the presence of auxin, TIR1 and AFB2 form specific sensing complexes with IAA6,
61 IAA9 and/or IAA17 that modulate JA homeostasis to control AR initiation.

62

63 **Key words:** TIR1/AFB, AuxIAA, jasmonate, adventitious roots, Arabidopsis

64

65 INTRODUCTION

66 In *Arabidopsis thaliana*, auxin-dependent gene regulation is mediated by the 23 members of
67 the AUXIN RESPONSE FACTOR (ARF) family of transcription factors, which can either
68 activate or repress transcription (Okushima et al., 2005; reviewed in Chapman and Estelle,
69 2009 and Guilfoyle and Hagen, 2007). Interaction studies have shown that most of the 29
70 auxin/indole-3-acetic acid (Aux/IAA) inducible proteins can interact with ARF activators
71 (reviewed in Guilfoyle and Hagen, 2007; Vernoux et al., 2011). Aux/IAAs mediate
72 recruitment of the TOPLESS corepressor (Szemenyei et al., 2008) and act as repressors of
73 transcription of auxin-responsive genes. When the auxin level rises, it triggers interaction of
74 the two components of the auxin co-receptor complex, an F-box protein from the
75 TRANSPORT INHIBITOR1/AUXIN-SIGNALING F-BOX PROTEIN (TIR1/AFB) family
76 (Kepinski and Leyser 2005; Dharmasiri, et al. 2005a) and an Aux/IAA protein, promoting
77 ubiquitination and 26S-mediated degradation of the latter (Gray et al., 2001). Degradation of
78 the Aux/IAA protein releases the ARF activity and subsequent activation of the auxin-
79 responsive genes (reviewed in Wang and Estelle, 2014; Weijers and Wagner, 2016).
80 TIR1/AFBs show different affinities for the same Aux/IAA (Calderon Villalobos et al., 2012;
81 Parry et al., 2009), suggesting that different combinations of TIR1/AFB receptors may
82 partially account for the diversity of auxin response. In addition, it has been shown that most
83 Aux/IAAs can interact with many Aux/IAAs and ARFs in a combinatorial manner, increasing
84 the diversity of possible auxin signaling pathways that control many aspects of plant
85 development and physiology (Boer et al., 2014; reviewed in Guilfoyle and Hagen, 2012;
86 Korasick et al., 2014; Nanao et al., 2014; Vernoux et al., 2011; Weijers et al., 2005). Several
87 studies have suggested specialized functions for some of the ARF and IAA combinations
88 during embryo development (Hamann et al., 2002), lateral root (LR) development (De Rybel
89 et al., 2010; De Smet et al., 2010; Fukaki et al., 2002; Lavenus et al., 2013; Tatematsu et al.,
90 2004), phototropism (Sun et al., 2013) and fruit development (Wang et al., 2005). However,
91 most of these studies involved characterization of gain-of-function stabilizing mutations,
92 which limited identification of more specialized functions for individual Aux/IAA genes. To
93 date, genetic investigations of Aux/IAA genes have been hampered by the lack of obvious
94 phenotype in the loss-of-function mutants (Overvoorde et al., 2005). Nevertheless, recent
95 careful characterization of a few of the mutants identified more precise functions in primary
96 or LR development for *IAA3* or *IAA8* (Arase et al., 2012; Dello Ioio et al., 2008) or in the
97 response to environmental stresses for *IAA3*, *IAA5*, *IAA6* and *IAA19* (Orosa-Puente et al.,
98 2018; Shani et al., 2017).

99 To decipher the role of auxin in the control of adventitious root (AR) development, which is a
100 complex trait with high phenotypic plasticity (reviewed in Bellini et al., 2014 and Geiss et al.,
101 2009), we previously identified a regulatory module composed of three *ARF* genes (two
102 activators *ARF6* and *ARF8*, and one repressor *ARF17*) and their regulatory microRNAs
103 (miR167 and miR160) (Gutierrez et al., 2009). These genes display overlapping expression
104 domains, interact genetically and regulate each other's expression at transcriptional and post-
105 transcriptional levels by modulating the availability of their regulatory microRNAs miR160
106 and miR167 (Gutierrez et al., 2009). The three ARFs control the expression of three auxin
107 inducible *Gretchen Hagen 3 (GH3)* genes encoding acyl-acid-amido synthetases (GH3.3,
108 GH3.5 and GH3.6) that, in addition to inactivating IAA (Staswick et al., 2005), inactivate
109 jasmonic acid (JA), an inhibitor of AR initiation in *Arabidopsis* hypocotyls (Gutierrez et al.,
110 2012; Supplemental Figure 1A). In a yeast two-hybrid system, ARF6 and ARF8 proteins were
111 shown to interact with almost all Aux/IAA proteins (Vernoux et al., 2011). Therefore, we
112 propose a model in which increased auxin levels facilitate formation of a coreceptor complex
113 with at least one TIR1/AFB protein and subsequent degradation of Aux/IAs (Supplemental
114 Figure 1B), thereby releasing the activity of ARF6 and ARF8 and the transcription of *GH3*
115 genes. In the present work, we describe identification of members of the potential co-receptor
116 complexes involved in this pathway. Using loss-of-function mutants, we demonstrate that
117 *TIR1* and *AFB2* are positive regulators, whereas *IAA6*, *IAA9* and *IAA17* are negative
118 regulators of AR formation. We suggest that TIR1 and AFB2 form co-receptor complexes
119 with at least three Aux/IAA proteins (*IAA6*, *IAA9* and *IAA17*), which negatively control
120 *GH3.3*, *GH3.5* and *GH3.6* expression by repressing the transcriptional activity of ARF6 and
121 ARF8, thereby modulating JA homeostasis and consequent AR initiation. In addition, we
122 show that several genes involved in JA biosynthesis are upregulated in the *tir1-1* mutant,
123 suggesting a probable dual role of TIR1 in both the biosynthesis and conjugation of
124 jasmonate.

125

126 **RESULTS**

127 **TIR1 and AFB2 but not other AFB proteins control adventitious root initiation in** 128 ***Arabidopsis* hypocotyls**

129 To assess the potential contributions of different TIR/AFB proteins to regulation of
130 adventitious rooting in *Arabidopsis*, we analyzed AR formation in *tir1-1*, *afb1-3*, *afb2-3*,
131 *afb3-4*, *afb4-8*, *afb5-5* single knockout (KO) mutants, double and triple mutants using
132 previously described conditions ((Gutierrez et al., 2009; Sorin et al., 2005) and Figure 1A).

133 The average number of ARs developed by *afb1-3*, *afb3-4*, *afb4-8*, *afb5-5* single mutants and
134 *afb4-8afb5-5* double mutants did not differ significantly from the average number developed
135 by wild-type seedlings (Figure 1A). These results suggest that AFB1, AFB3, AFB4 and
136 AFB5 do not play a significant role in AR initiation. In contrast, *tir1-1* and *afb2-3* single
137 mutants produced 50% fewer ARs than the wild-type plants and the *tir1-1afb2-3* double
138 mutant produced even fewer, indicating an additive effect of the mutations (Figure 1A). The
139 *afb1-3afb2-3* and *afb2-3afb3-4* double mutants retained the same phenotype as the *afb2-3*
140 single mutant, and the triple mutant *tir1-1afb1-3and afb3-4* had the same phenotype as the
141 *tir1-1* single mutant confirming a minor role, if any, of AFB1 and AFB3 in AR initiation. We
142 also checked the root phenotype of the *tir1-1* and *afb2-3* single mutants and *tir1-1afb2-3*
143 double mutant under the growth conditions used. No significant differences were observed in
144 the primary root length (Supplemental Figure 2A), but the number of LRs was slightly but
145 significantly decreased in both the *tir1-1* and *afb2-3* single mutants and dramatically
146 decreased in the double mutant (Supplemental Figure 2B), as already shown by others
147 (Dharmasiri et al., 2005b; Parry et al., 2009, Xuan et al., 2015). This resulted in a reduction of
148 the LR density in all genotypes (Supplemental Figure 2C), confirming the additive and
149 pleiotropic role of the TIR1 and AFB2 proteins. In order to confirm that the growth
150 conditions we used to induce ARs did not compromise the root development compared to the
151 canonical conditions used to study LR development, we performed similar experiments with
152 seedlings grown in the light for ten days and obtained similar results (Supplemental Figure
153 2J-L)

154

155 **TIR1 and AFB2 proteins are expressed in young seedlings during AR initiation**

156 To analyze the expression pattern of the TIR1 and AFB2 proteins during the early
157 stages of AR initiation and development, plants expressing the translational fusions
158 *pTIR:cTIR1:GUS* or *pAFB2:cAFB2:GUS* were grown as previously described (Gutierrez et
159 al., 2009). At time 0 (T0), i.e., in etiolated seedlings just before transfer to the light, the
160 TIR1:GUS and AFB2:GUS proteins were strongly expressed in the root apical meristem,
161 apical hook and cotyledons. Interestingly AFB2:GUS was also detected in the vascular
162 system of the root and the hypocotyl, whereas TIR1:GUS was not detectable in those organs
163 (Figure 1B). Nine hours after transfer to the light, TIR1:GUS protein disappeared from the
164 cotyledons but was still strongly expressed in the shoot and root meristems. Its expression
165 was increased slightly in the upper part of the hypocotyl. In contrast, AFB2:GUS was still
166 highly detectable in the shoot and root meristems, cotyledons and vascular system of the root.

167 In addition, its expression was induced throughout almost the entire hypocotyl (Figure 1B).
168 Seventy-two hours after transfer to the light, TIR1:GUS and AFB2:GUS showed almost the
169 same expression pattern, which was reminiscent of that previously described in light grown
170 seedlings (Parry et al., 2009). None of the proteins were detectable in the cotyledons.
171 However, they were present in the shoot meristem and young leaves and the apical root
172 meristem. In the hypocotyl and root, the TIR1:GUS and AFB2:GUS proteins were mainly
173 detectable in the AR and LR primordia (Figure 1B). Although we did not observe any
174 obvious phenotype in the knock out mutants for the AFB1, AFB3, AFB4 and AFB5 proteins
175 we checked their expression during AR initiation using translational fusion lines
176 (Supplemental Figure 3). AFB4:GUS was not at all detected in young seedlings, neither in the
177 dark (Supplemental Figure 3A) nor after transfer to the light for 9 or 72 h (Supplemental
178 Figure 3B and C). AFB5:GUS showed similar profile except an expression in the cotyledons
179 and the root tip in all conditions (Supplemental Figure 3). After transfer to the light the
180 expression of AFB5:GUS extended slightly to the top of the hypocotyl. The absence or very
181 low abundance of AFB4 and AFB5 proteins in the hypocotyl can explain the absence of
182 phenotype in the corresponding mutants and let us conclude that these two proteins do not
183 play a role in the control of AR initiation. In contrast, AFB1:GUS was highly accumulating in
184 the whole seedling at T0 and after transfer to the light (Supplemental Figure 3). Although at a
185 lower level, the AFB3:GUS showed similar expression profile as AFB1 but its level
186 decreased after transfer to the light (Supplemental Figure 3). The absence of phenotype in the
187 *afb1-3* and *afb3-4* loss-of-function mutants cannot be explained by the absence of the proteins
188 but likely by the fact they either target other signaling pathways not related to AR initiation or
189 because they have a very low affinity for the Aux/IAA proteins involved in this process. It
190 was indeed shown that TIR1 and AFB2 exhibit a stronger interaction with selected Aux/IAA
191 than AFB1 and AFB3 (Parry et al., 2009) and that AFB1 and AFB3 had little effect on auxin-
192 dependent Aux/IAA degradation (Havens et al., 2012). Therefore, we conclude that TIR1 and
193 AFB2 are the main Auxin F-box proteins involved in the control of AR initiation.

194

195 **TIR1 likely controls both JA biosynthesis and conjugation, whereas AFB2 preferentially**
196 **controls JA conjugation during adventitious root initiation**

197 We previously reported that the AR phenotype was positively correlated with either the
198 amount of GH3 (GH3.3, GH3.5 and GH3.6) proteins (Sorin et al. 2006) or their relative
199 transcript amount (Gutierrez et al., 2012; Pacurar et al., 2014a), therefore based on our model
200 (Supplemental Figure 1A and B), one would expect to see a reduction of the relative transcript

201 amount of the *GH3* genes in the *tir1-1*, *afb2-3* single mutants and *tir1-1afb2-3* double mutant.
202 Therefore, we analyzed the relative transcript amount of the three *GH3* genes in these mutants
203 (Figure 1C). *GH3-11/JAR1*, which conjugates JA into its bioactive form jasmonoyl-L-
204 isoleucine (JA-Ile), was used as a control. Its expression was only slightly downregulated
205 (40% compared to the wild type) in the *afb2-3* single mutant and *tir1-1afb2-3* double mutant
206 at T72 (Figure 1C), whereas the relative transcript amount of the *GH3* genes was significantly
207 reduced in the *afb2-3* single mutant and *tir1-1afb2-3* double mutant at different time points
208 (Figure 1C).

209 At T0 only *GH3.3* was significantly downregulated (73% relatively to the wild type) in *tir1-1*
210 while the three *GH3* genes were downregulated in *afb2-3* single mutant (Figure 1C). An
211 additive effect of *tir1-1* mutation was observed for the downregulation of *GH3.3* in the *tir1-1*
212 *afb2-3* double mutant.

213 At T9, *GH3.5* and *GH3.6* were significantly downregulated (60% and 40% relatively to the
214 wild type respectively) in *afb2-3* mutant. In contrast, except *GH3.3* which was slightly
215 upregulated (40% relatively to the wild type) in *tir1-1*, the relative transcript amount of the
216 other two genes was unaffected in this mutant. Nevertheless, in the double mutant *tir1-1afb2-3*
217 the relative transcript amount of *GH3.3* and *GH3.5* was significantly decreased compared to
218 the single *afb2-3* mutant suggesting a synergistic effect of the *tir1-1* mutation at this time
219 point.

220 At T72, only *GH3.3* was slightly (35%) but significantly downregulated in *tir1-1* mutant,
221 while the three *GH3* genes were downregulated in *afb2-3*. As at T9, the relative transcript
222 amount of the *GH3* genes was more affected in the *tir1-1afb2-3* double mutant than in the
223 *afb2-3* single suggesting again a synergistic effect of the two mutations at T72 (Figure 1C).

224 In conclusion, the relative transcript amount of the *GH3* genes is significantly affected in the
225 *afb2-3* single mutant at all time points, strongly suggesting that AFB2 likely controls AR
226 initiation by regulating JA homeostasis through the *ARF6/ARF8* auxin signaling module (as
227 shown in Supplemental Figure 1). The role of TIR1 in the control of JA conjugation is not as
228 clear, but the synergistic effect on the expression of the *GH3* genes in the double mutant at T9
229 and T72 suggests that in certain circumstances it also plays a role.

230 Because AR initiation is affected at the same level in both *tir1-1* and *afb2-3* mutant lines, we
231 hypothesized that TIR1, besides its redundant function in JA conjugation, might have another
232 role in controlling AR initiation by regulating other hormone biosynthesis and/or signaling
233 cascades. To test this hypothesis, we quantified endogenous free salicylic acid (SA), free
234 IAA, free JA and JA-Ile (Figure 2A to D) in the hypocotyls of wild-type seedlings and

235 seedlings of the *tir1-1*, *afb2-3* single mutants and *tir1-1afb2-3* double mutant. No significant
236 differences in SA content were observed between the wild type and mutants (Figure 2A). A
237 significant increase in free IAA content was observed at T0 in all three mutants compared to
238 the wild type (25% in *tir1-1* and *afb2-3*; 50% in the double mutant; Figure 2B), but only in
239 the *tir1-1afb2-3* double mutant at 9 and 72 hours after transfer to the light (42% increase at T9
240 and 33% T72; Figure 2B). Takato et al. (2017) have shown that auxin biosynthesis is
241 repressed in a feedback manner by the Aux/IAA and SCF^{TIR1/AFB}-mediated auxin-signaling
242 pathway. Therefore, we conclude that the increase in the free IAA content we observed in the
243 *tir1-1*, *afb2-3* single and *tir1-1afb2-3* double mutants can be explained as a consequence of
244 the downregulation of the auxin signaling pathway which cannot repress the biosynthesis in
245 the mutants

246 At T0 and T9, a significant increase in free JA was observed in both the *tir1-1* and *afb2-3*
247 single mutants (47% for *tir1-1* and 50% for *afb2-3* at T0; 43% for *tir1-1* and 40% for *afb2-3*
248 at T9) compared to the wild type but not in the double mutant *tir1-1afb2-3* (Figure 2C). The
249 bioactive form JA-Ile was significantly accumulated in the single mutants at all three time
250 points but accumulated only at T9 in the double mutant *tir1-1afb2-3* (Figure 2D).
251 Accumulation of JA and JA-Ile in the *afb2-3* mutant was expected since the three GH3
252 conjugating enzymes were found to be downregulated (Figure 1C), but we did not *a priori*
253 expect the same level of accumulation for the *tir1-1* mutant which is not strongly affected in
254 the expression of *GH3* genes. Accumulation of JA can be due to a reduction of its conjugation
255 by the GH3 proteins but also to an increase of its biosynthesis. Interestingly it was previously
256 shown that flower buds of auxin receptor mutants produced more JA than the wild-type plants
257 (Cecchetti et al., 2013). Therefore, we checked the expression of JA biosynthesis genes in the
258 mutants to investigate the potential role of TIR1 and/or AFB2 in the control of JA
259 biosynthesis. The relative transcript amounts of seven key genes involved in JA biosynthesis
260 were analyzed by qRT-PCR in the hypocotyls of wild-type, *tir1-1*, *afb2-3* and *tir1-1afb2-3*
261 seedlings grown under adventitious rooting conditions (Figure 3A to C).

262 At T0, *OPCLI*, *OPR3*, *AOC2* were significantly upregulated (60%, 55% and 73 %
263 respectively relative to the wild type) in the *tir1-1* mutant compared to the wild type, whereas
264 *LOX2* was downregulated (70% relative to the wild type). In the *afb2-3* mutant, no significant
265 differences were observed except for *LOX2* and *AOC1*, which were downregulated compared
266 to the wild type. In the double mutant, *LOX2* and *AOC2* were significantly upregulated
267 (Figure 3A).

268 Nine hours after transfer to the light (T9), five (*OPCLI*, *OPR3*, *LOX2*, *AOC2*, *AOC3*) out of

269 the seven biosynthesis genes were significantly upregulated in the single *tir1-1* mutant and
270 four of them (*OPCLI*, *OPR3*, *LOX2*, *AOC2*) were upregulated in the *tir1-1afb2-3* double
271 mutant (Figure 3B), while only *AOC3* and *AOC4* were upregulated in the *afb2-3* mutant
272 (Figure 3B). At T72, only *LOX2* was significantly upregulated in all three mutants (Figure
273 3C). In conclusion, the *tir1-1* mutation alone has little effect on the expression of the *GH3*
274 genes involved in the conjugation of JA (Figure 1C) but a significant positive effect on the
275 expression of JA biosynthetic genes at T0 and T9. In contrast the *afb2-3* mutation induced a
276 significant downregulation of the *GH3* genes at all time points (Figure 1C) but has little effect
277 on the expression of the JA biosynthesis genes (Figure 3). In addition, we observed a
278 synergistic effect of *tir1-1* mutation when combined with the *afb2-3* mutation since the *GH3*
279 genes were more downregulated in the double mutant than in the single *afb2-3* mutant,
280 suggesting that, in certain circumstances, TIR1 might play a role in the conjugation of JA
281 through the GH3 proteins

282 The fact that JA and JA-Ile did not accumulate in the double mutant is intriguing as an
283 upregulation of the biosynthesis pathway combined to a downregulation of the conjugation
284 should in contrast lead to an accumulation of JA and JA-Ile. Because too much JA and JA-Ile
285 might become deleterious for the plant, as they inhibit most of the growth processes
286 (reviewed in Huang et al., 2017) a negative feedback loop regulating JA homeostasis by
287 might be set up by the plant to induce the degradation of JA in order to maintain a steady state
288 level. Although significant progress has been made in identifying pathways involved in JA
289 metabolism, their regulation is still poorly understood, and more research is needed to
290 decipher the complexity of these pathways (reviewed in Wasternack and Feussner, 2017)

291 Therefore, we propose that both TIR1 and AFB2 control JA homeostasis during AR initiation,
292 with a dual role for TIR1 in the control of JA biosynthesis through a pathway yet to be
293 identified and/or conjugation through the *ARF6/ARF8* auxin signaling module depending on
294 the development stage, and a major role for AFB2 in the control of JA conjugation through
295 the *ARF6/ARF8* auxin signaling module.

296

297 ***IAA6*, *IAA9* and *IAA17* act redundantly to control adventitious root initiation**

298 ARF6 and ARF8 are two positive regulators of AR initiation (Gutierrez et al., 2009;
299 Gutierrez et al., 2012) and their transcriptional activity is known to be regulated by Aux/IAA
300 genes. To gain further insight into the auxin sensing machinery and complete our proposed
301 signaling module involved in AR initiation, we attempted to identify potential Aux/IAA
302 proteins that interact with ARF6 and/or ARF8. In 2011, Vernoux *et al.* (2011) conducted a

303 large-scale analysis of the Aux/IAA-ARF network using a high-throughput yeast two-hybrid
304 approach. They showed that ARF6 and ARF8 belong to a cluster of proteins that can interact
305 with 22 of the 29 Aux/IAA genes (Vernoux et al., 2011). However, this does not help much to
306 restrict the number of genes of interest. Hence, to elucidate which Aux/IAs can interact with
307 ARF6 and ARF8 during AR formation, we looked at those most expressed in the hypocotyl
308 and assessed the expression of the 29 *Aux/IAA* genes in different organs (cotyledons,
309 hypocotyl and roots) of 7-day-old light-grown seedlings using qRT-PCR (Supplemental
310 Figure 4). With the exception of *IAA15*, we detected a transcript for all *IAA* genes in all
311 organs tested (Supplemental Figure 4). Genes with similar expression levels between organs
312 were clustered based on Pearson's correlation, and we observed that, although they were all
313 expressed in the three organs, the profile of expression varied. We observed that 18 *IAA* genes
314 were more expressed in the hypocotyl relatively to cotyledons or roots (*IAA1*, *IAA2*, *IAA3*,
315 *IAA4*, *IAA5*, *IAA6*, *IAA7*, *IAA8*, *IAA9*, *IAA10*, *IAA13*, *IAA14*, *IAA16*, *IAA19*, *IAA26*, *IAA27*,
316 *IAA30*, *IAA31*), 4 *IAA* genes were more expressed in the hypocotyl and the root (*IAA17*,
317 *IAA20*, *IAA28*, *IAA33*) and 6 genes were more expressed in the cotyledons (*IAA11*, *IAA12*,
318 *IAA18*, *IAA29*, *IAA32*, *IAA34*). This differences in the expression pattern certainly contributes
319 to drive a certain specificity of action among the highly redundant *Aux/IAA* genes. To assess
320 the potential contributions of different *IAA* genes in the regulation of AR, we obtained KO
321 mutants available for nine of the *Aux/IAA* genes that displayed a relatively higher expression
322 in the hypocotyl compared to the cotyledons (*iaa3/shy2-24*, *iaa4-1*, *iaa5-1*, *iaa6-1*, *iaa7-1*,
323 *iaa8-1*, *iaa9-1*, *iaa14-1*, *iaa30-1*), two of the genes which had a higher expression in both the
324 hypocotyl and root (*iaa17-6*, *iaa28-1*, *iaa33-1*) and we added two KO mutants with genes
325 whose expression was lower in the hypocotyl and root (*iaa12-1* and *iaa29-1*).

326 We analyzed AR formation in the *iaa* KO mutants under previously described conditions
327 (Gutierrez et al., 2009; Sorin et al., 2005). Interestingly, six mutants (*iaa5-1*, *iaa6-1*, *iaa7-1*,
328 *iaa8-1*, *iaa9-1* and *iaa17-6*) produced significantly more ARs than the wild type, whereas all
329 the other mutants did not show any significant difference compared to the wild type (Figure
330 4A). The primary root length and LR number were not affected in mutants *iaa5-1*, *iaa6-1* and
331 *iaa8-1* (Supplemental Figure 2D to F), whereas *iaa9-1* and *iaa17-6* showed a slightly shorter
332 primary root and fewer LRs than the wild type (Supplemental Figure 2D and E) but the LR
333 density was not affected (Supplemental Figure 2F). In contrast, *iaa7-1* had a slightly but
334 significantly longer primary root as well as fewer LRs, which led to a slightly but
335 significantly decreased LR density (Supplemental Figure 2F). These results strongly suggest
336 that *IAA5*, *IAA6*, *IAA7*, *IAA8*, *IAA9* and *IAA17* are involved in the control of AR formation

337 and substantiate our hypothesis that only a subset of *Aux/IAA* genes regulate the process of
338 AR formation.

339 Because we found an interaction with ARF6 and/or ARF8 only with the IAA6, IAA9
340 and IAA17 proteins (see below), we continued to characterize the role of their corresponding
341 genes. All three single *iaa* mutants showed a significant and reproducible AR phenotype.
342 Nevertheless, because extensive functional redundancy has been shown among *Aux/IAA* gene
343 family members (Overvoorde et al., 2005), it was important to confirm the phenotype in at
344 least a second allele (Figure 4B). We also generated the double mutants *iaa6-liaa9-1*, *iaa6-*
345 *liaa17-6* and *iaa9-liaa17-6* and the triple mutant *iaa6-liaa9-liaa17-6* and analyzed their
346 phenotype during AR formation (Figure 4C). Mutant *iaa4-1* was used as a control showing no
347 AR phenotype. Except for the *iaa6liaa17-6* double mutant, which showed an increased
348 number of AR compared to the single mutants, the other two double mutants were not
349 significantly different from the single mutants (Figure 4C). Nevertheless, we observed a
350 significant increase of the AR number in the triple mutants compared to the double mutants,
351 suggesting that these genes act redundantly in the control of AR initiation (Figure 4C) but do
352 not seem to be involved in the control of the PR or LR root growth as shown on
353 (Supplemental Figure 2G-I). Again, in order to confirm that the growth conditions set for AR
354 initiation do not affect LR development we also analyze the PR and LR development of the
355 triple mutant *iaa6-liaa9-liaa17-6* grown in light conditions only (Supplemental Figure 2J-L)
356 and confirmed the absence of PR and LR phenotype.

357 We also characterized the expression of *IAA6*, *IAA9* and *IAA17* during the early steps of AR
358 formation using transcriptional fusion constructs containing a β -glucuronidase (*GUS*) coding
359 sequence fused to the respective promoters. At time T0 (i.e., etiolated seedlings prior to
360 transfer to the light) (Figure 4D), *promIAA6:GUS* was strongly expressed in the hypocotyl,
361 slightly less expressed in the cotyledons and only weakly expressed in the root;
362 *promIAA9:GUS* was strongly expressed in the cotyledons, hook and root tips and slightly less
363 in the hypocotyl and root; *promIAA17:GUS* was strongly expressed in the hypocotyl and root,
364 slightly less in the cotyledons and, interestingly, was excluded from the apical hook (Figure
365 4D). Forty-eight and seventy-two hours after transfer to the light, a decrease in *GUS* staining
366 was observed for all the lines (Figure 4F and H), but only for *IAA9* when the seedlings were
367 kept longer in the dark (Figure 4E and G). These results suggest that light negatively regulates
368 the expression of *IAA6* and *IAA17* while the expression of *IAA9* seem to depend on the
369 developmental stage.

370

371 **IAA6, IAA9 and IAA17 proteins interact with ARF6 and ARF8 proteins**

372 To establish whether these targeted proteins were effective partners of ARF6 and
373 ARF8, we performed co-immunoprecipitation (CoIP) in protoplasts transfection assays.
374 Arabidopsis protoplasts were transfected with plasmids expressing cMyc- or HA-tagged
375 AuxIAA and ARF proteins according to the protocol described in the Materials and Methods
376 (Magyar et al., 2005). The presence of the putative ARF/AuxIAA complex was tested by
377 western blotting with anti-HA or anti-c-Myc antibodies and only interactions with *IAA6*, *IAA9*
378 and *IAA17* were detected (Figure 5A to E): *IAA6* and *IAA17* interacted with ARF6 and ARF8
379 (Fig. 5A, B, D and E), whereas *IAA9* interacted only with ARF8 (Figure 5C). These results
380 were confirmed by a bimolecular fluorescence complementation (BiFC) assay (Figure 5I to
381 M)

382

383 **ARF6 but not ARF8 can form a homodimer**

384 Recent interaction and crystallization studies have shown that ARF proteins dimerize
385 *via* their DNA-binding domain (Boer et al., 2014) and interact not only with Aux/IAA
386 proteins but potentially also with themselves or other ARFs *via* their PB1 domain with a
387 certain specificity (Vernoux et al., 2011). Therefore, we also used CoIP and BiFC assays and
388 tagged versions of the ARF6 and ARF8 proteins to check whether they could form
389 homodimers and/or a heterodimer. Our results (Figure 5G, H, O and P) agreed with a
390 previously published yeast two-hybrid interaction study (Vernoux et al., 2011), which showed
391 that ARF6 and ARF8 do not interact to form a heterodimer and that ARF8 does not
392 homodimerize. In contrast, we showed that ARF6 protein can form a homodimer (Figure 5F
393 and N), suggesting that ARF6 and ARF8, although redundant in controlling the expression of
394 *GH3.3*, *GH3.5* and *GH3.6* genes (Gutierrez et al., 2012), might have a specificity of action.

395

396 ***ARF6*, *ARF8* and *ARF17* are unstable proteins and their degradation is proteasome
397 dependent**

398 While transfecting Arabidopsis protoplasts for CoIP assays with open reading frames
399 encoding individual cMyc- or HA-tagged versions of ARFs and Aux/IAs, problems were
400 encountered due to instability not only of the tagged Aux/IAA proteins but also of the tagged
401 ARFs. It has previously been reported that like Aux/IAA proteins, ARFs may be rapidly
402 degraded (Salmon et al., 2008). Therefore, we analyzed the degradation of HA₃:ARF6,
403 cMyc₃:ARF8 and HA₃:ARF17. We used HA₃:ARF1, which was previously used as a control
404 (Figure 6A,E,F) (Salmon et al., 2008). Western blot analysis with protein extracts from

405 transfected protoplasts using anti-HA or anti-cMyc antibodies showed that like ARF1,
406 proteins ARF6, ARF8 and ARF17 were degraded. The HA₃:ARF6 levels decreased
407 dramatically within 30 minutes, indicating that ARF6 is a short-lived protein (Figure 6B),
408 while the degradation rate of HA₃:ARF17 was similar to that of HA₃:ARF1 (Figure 6D) and
409 cMyc₃ARF8 appeared more stable (Figure 6C). To verify whether ARF6, ARF8 and ARF17
410 proteolysis requires activity of the proteasome for proper degradation, transfected protoplasts
411 were incubated for 2 h in the presence or absence of 50 μM of a cell permeable proteasome-
412 specific inhibitor, Z-Leu-Leu-Leu- CHO aldehyde (MG132), and the extracted proteins were
413 analyzed by immunoblotting (Figure 6E). The sample incubated with MG132 contained
414 higher levels of HA₃:ARF1, confirming the previously described proteasome-dependent
415 degradation of ARF1 (Salmon et al., 2008), and thereby the efficiency of the treatment.
416 Similarly, HA₃:ARF6, cMyc₃ARF8 and HA₃:ARF17 proteins accumulated in protoplasts
417 treated with MG132, indicating that ARF6, ARF8 and ARF17 degradation is also proteasome
418 dependent (Figure 6E). To further determine whether proteasome activity is necessary for
419 ARF6, ARF8 and ARF17 protein degradation *in vivo*, one-week-old transgenic *in vitro* grown
420 Arabidopsis seedlings expressing HA₃:ARF1, cMyc₃:ARF6, cMyc₃:ARF8 and cMyc₃:ARF17
421 were treated with MG132 or DMSO for 2 h prior to protein extraction. After western blotting,
422 we observed that levels of HA₃:ARF1, cMyc₃:ARF6, cMyc₃:ARF8 and cMyc₃:ARF17 were
423 enhanced by the addition MG132, confirming that their degradation is proteasome dependent
424 in planta (Figure 6F).

425

426 ***IAA6, IAA9 and IAA17* negatively control expression of *GH3.3, GH3.5 and GH3.6***

427 In our model, auxin stimulates adventitious rooting by inducing *GH3.3, GH3.5* and
428 *GH3.6* gene expression *via* the positive regulators ARF6 and ARF8 (Supplemental Figure 1).
429 Although we confirmed an interaction between IAA6, IAA9 and IAA17 with ARF6 and/or
430 ARF8, it was important to demonstrate whether disrupting the expression of one of those
431 genes would result in upregulation of *GH3* gene expression. Therefore, we performed qRT-
432 PCR analysis of the relative transcript amounts of the three genes *GH3.3, GH3.5, GH3.6* in
433 the hypocotyls of single mutants *iaa6-1, iaa9-1, iaa17-6* first etiolated and then transferred to
434 the light for 72 h. The mutant *iaa4.1*, which had no phenotype affecting AR initiation (Figure
435 4A), was used as a control. Expression of *GH3.3, GH3.5* and *GH3.6* was upregulated in the
436 *iaa9-1* mutant (Figure 7A), whereas only *GH3.3, GH3.5* were significantly upregulated in the
437 *iaa6-1* and *iaa17-6* mutant (Figure 7A). In contrast, expression of *GH3.3, GH3.5* and *GH3.6*
438 remained unchanged in the *iaa4-1* mutant (Figure 7A). These results confirm that IAA6,

439 IAA9 and IAA17 are involved in the regulation of adventitious rooting through the
440 modulation of *GH3.3*, *GH3.5* and *GH3.6* expression. To establish whether the *iaa6-1*, *iaa9-1*
441 and *iaa17-6* mutations affected other *GH3* genes, the relative transcript amount of *GH3-10*
442 and *GH3-11* was quantified. Notably, accumulation of *GH3.10* and *GH3.11/JAR1* transcripts
443 was not significantly altered in the *iaa6-1*, *iaa9-1* and *iaa17-6* mutants but *GH3.10* was
444 upregulated in the *iaa4-1* mutant (Figure 7A). We concluded that *IAA6*, *IAA9* and *IAA17*
445 negatively regulate *GH3.3*, *GH3.5* and *GH3.6* expression in the Arabidopsis hypocotyl during
446 AR initiation.

447 We also checked a possible compensatory effect induced by the knockout of one the
448 IAA genes. We performed qRT-PCR analysis of the relative transcript amounts of *IAA6*, *IAA9*
449 and *IAA17* genes in the hypocotyl of each single mutant (Figure 7B). Interestingly, a mutation
450 in the *IAA6* gene did not affect the expression of *IAA9* or *IAA17*, whereas *IAA17* was
451 significantly upregulated in the hypocotyls of *iaa9-1* mutant seedlings. *IAA6* was upregulated
452 in the hypocotyl of *iaa17-6* mutant seedlings and a mutation in *IAA4* did not affect the
453 expression of any of the three IAA genes of interest (Figure 7B).

454

455 **DISCUSSION**

456 AR formation is a post-embryonic process that is intrinsic to the normal development
457 of monocots. In both monocots and dicots, it can be induced in response to diverse
458 environmental and physiological stimuli or through horticultural practices used for vegetative
459 propagation of many dicotyledonous species (reviewed in (Bellini et al., 2014; Steffens and
460 Rasmussen, 2016)). Vegetative propagation is widely used in horticulture and forestry for
461 amplification of elite genotypes obtained in breeding programs or selected from natural
462 populations. Although this requires effective rooting of stem cuttings, this is often not
463 achieved, and many studies conducted at physiological, biochemical and molecular levels to
464 better understand the entire process have shown that AR formation is a heritable quantitative
465 genetic trait controlled by multiple endogenous and environmental factors. In particular, it has
466 been shown to be controlled by complex hormone cross-talks, in which auxin plays a central
467 role (reviewed in (Lakehal and Bellini, 2019; Pacurar et al., 2014b)). The specificity of auxin
468 response is thought to depend on a specific combinatorial suite of ARF–Aux/IAA protein–
469 protein interactions from among the huge number of potential interactions that modulate the
470 auxin response of gene promoters via different affinities and activities (reviewed in (Vernoux
471 et al., 2011; Weijers et al., 2005)). In previous work, we identified a regulatory module
472 composed of three *ARF* genes, two activators (*ARF6* and *ARF8*) and one repressor (*ARF17*),

473 which we showed could control AR formation in Arabidopsis hypocotyls (Gutierrez et al.,
474 2009) (Supplemental Figure 1). Recent developments have highlighted the complexity of
475 many aspects of ARF function. In particular, crystallization of the DNA binding domains of
476 ARF1 and ARF5 (Boer et al., 2014) and the C-terminal protein binding domain 1 (PB1) from
477 ARF5 (Nanao et al., 2014) and ARF7 (Korasick et al., 2014) has provided insights into the
478 physical aspects of ARF interactions and demonstrated new perspectives for dimerization and
479 oligomerization that impact ARF functional cooperativity (Parcy et al., 2016). Here, we
480 provide evidence that ARF6 can form a homodimer while we could detect neither
481 heterodimerization between ARF6 and ARF8 nor ARF8 homodimerization. How this
482 influences their respective role in the control of AR initiation is not yet known and requires
483 further investigation. Nevertheless, based on a recent structural analysis of other ARFs (Boer
484 et al., 2014; Parcy et al., 2016), we propose that the ARF6 homodimer would probably target
485 different sites from that of a monomeric ARF8 protein in the *GH3s* promoters, and/or that
486 their respective efficiency of transcriptional regulation would be different, suggesting that one
487 of the two transcription factors might have a prevalent role compared to the other. The
488 prevailing model for auxin-mediated regulation of the Aux/IAA–ARF transcriptional complex
489 is *via* increased Aux/IAA degradation in the presence of auxin, permitting ARF action,
490 possibly through ARF-ARF dimerization, and subsequent regulation of auxin-responsive
491 genes (Nanao et al., 2014; Parcy et al., 2016). As a further step of regulation for auxin-
492 responsive gene transcription, it has been suggested that proteasomal degradation of ARF
493 proteins may be as important as that of Aux/IAA proteins to modulate the ratio between ARFs
494 and Aux/IAAs proteins (Salmon et al., 2008). In the present work, we demonstrated that like
495 ARF1 (Salmon et al., 2008), proteins ARF6, ARF8 and ARF17 undergo proteasome
496 dependent degradation. We previously showed that the balance between the two positive
497 regulators ARF6 and ARF8 and the negative regulator ARF17 was important for determining
498 the number of ARs and that this balance was modulated at the post-transcriptional level by the
499 action of the microRNAs miR167 and miR160 (Gutierrez et al., 2009). Here, we suggest that
500 the proteasome dependent degradation of ARF6, ARF8 and ARF17 proteins is an additional
501 level of regulation for modulation of the transcription factor balance during AR formation.

502 ARF6 and ARF8 (but not ARF17) retain PB1 in their structure, which makes them
503 targets of Aux/IAA repressor proteins. Because most previous genetic studies of *Aux/IAA*
504 genes focused on characterization of gain-of-function mutants and there are only a few recent
505 characterizations of KO mutants (Arase et al., 2012; Shani et al., 2017), we attempted to
506 identify potential Aux/IAA partners involved in the control of AR initiation in the

507 *Arabidopsis* hypocotyl. Nevertheless, likely because AR formation is a quantitative trait, we
508 identified six *iaa* KO mutants showing an increased number of ARs. We confirmed direct
509 physical interaction with ARF6 and/or ARF8 for three of them (IAA6, IAA9 and IAA17) and
510 showed significant upregulation of *GH3.3*, *GH3.5* and *GH3.6* expression in the corresponding
511 single KO mutants, confirming that each of the three IAA proteins act as repressors in this
512 pathway. Vernoux *et al.* (2011) also showed interaction between IAA17 and the PB1 domain
513 of ARF6 and ARF8, but in contrast to our results, IAA9 was found to interact with ARF6 and
514 not ARF8. The same study showed interaction of ARF6 and ARF8 with IAA7 and IAA8,
515 which we did not observe when using the full-length proteins. Nevertheless, a KO mutation in
516 *IAA5*, *IAA7* and *IAA8* genes led to a similar phenotype as observed in *iaa6*, *iaa9* and *iaa17*
517 KO mutants. It is therefore possible that IAA5, IAA7 and IAA8 proteins contribute in a
518 combinatorial manner to generate a higher order of oligomerization through interaction with
519 one of the other three Aux/IAA proteins, leading to repression of ARF6 and ARF8 activity.
520 Indeed, Vernoux *et al.* (2011) showed that in the yeast two-hybrid interactome, IAA5, IAA7
521 and IAA8 interact with IAA6, IAA9 and IAA17. Further, recent work has demonstrated that
522 dimerization of the Aux/IAA repressor with the transcription factor is insufficient to repress
523 the activity and that multimerization is likely to be the mechanism for repressing ARF
524 transcriptional activity (Korasick *et al.*, 2014), which supports our hypothesis. Alternatively,
525 IAA5, IAA7 and IAA8 could contribute to repressing the activity of other ARFs, such as
526 ARF7 and/or ARF19, which have also been shown to be involved in the control of AR
527 formation (Sheng *et al.*, 2017).

528 In addition to Aux/IAA transcriptional repressors and ARF transcription factors,
529 TIR1/AFB F-box proteins are required for a proper auxin-dependent regulation of
530 transcription. Several elegant studies have shown that auxin promotes degradation of
531 Aux/IAA proteins through the SCF^{TIR1/AFB} in an auxin-dependent manner (Dharmasiri *et al.*,
532 2005a; Gray *et al.*, 2001; Kepinski and Leyser, 2005; Ramos *et al.*, 2001; Tan *et al.*, 2007).
533 Hence, our model would not be complete without the F-box proteins necessary to release
534 ARF6 and ARF8 transcriptional activity. Among the six TIR1/AFB proteins examined, we
535 demonstrated that TIR1 and AFB2 are the main players involved in this process. Both these
536 proteins act by modulating JA homeostasis since an accumulation of JA and JA-Ile was
537 observed in the single mutants. Nevertheless, our results suggest a different and
538 complementary role for TIR1 and AFB2. Indeed, a mutation in the *TIR1* gene did not affect
539 the expression of the three *GH3* genes in the same way as a mutation in the *AFB2* gene but
540 instead mainly affected the expression of genes involved in JA biosynthesis. These results are

541 in agreement with a previous study, which showed that TIR1 negatively controls JA
542 biosynthesis during flower development (Cecchetti et al., 2013). Similarly, the loss-of-
543 function *Osdao1* mutant in *Oryza sativa*, which accumulated significantly more free-IAA
544 than its wild type counterpart, was found to be defective in JA biosynthesis. All these results
545 indicate that TIR1-dependent auxin signaling may negatively control JA biosynthesis,
546 depending on the developmental stage (Zhao et al., 2013). ARF6 and ARF8 have also been
547 shown to be positive regulators of JA biosynthesis during flower development (Nagpal et al.,
548 2005). However, it is unlikely that TIR1 controls JA biosynthesis through ARF6 and/or ARF8
549 during AR initiation since ARF6 and ARF8 have been shown to be negative regulators of JA
550 accumulation and by this way positive regulators of AR initiation (Gutierrez et al., 2009;
551 Gutierrez et al., 2012). How TIR1-dependent auxin signaling negatively control JA
552 biosynthesis and which ARF(s) is (are) involved in this process is not known yet and requires
553 further investigation. We are conscious that both gene expression analysis and hormone
554 quantification were performed on whole hypocotyls, at particular time points and therefore
555 may not fully reflect the dynamic of events in the single cells from which the AR initiate.
556 Nevertheless, because our previous work had shown a clear correlation between *GH3* gene
557 expression or protein content in the whole hypocotyl and the number of ARs (Pacurar et al.,
558 2014a; Sorin et al., 2006) on a one hand, and that mutants deficient in JA biosynthesis had an
559 increased number of ARs (Gutierrez et al., 2012) on another hand, we would like to propose
560 here a dual role for TIR1 in the control of AR initiation, i.e., control of JA conjugation
561 through a ARF6/ARF8 signaling module and control of JA biosynthesis through a pathway
562 yet to be identified that would lead to similar amount of endogenous JA and JA isoleucine
563 depending on the developmental stage.

564 In conclusion, we propose that AR initiation in the Arabidopsis hypocotyl depends on
565 regulatory module comprising two F-box proteins (TIR1 and AFB2), at least three Aux/IAA
566 proteins (IAA6, IAA9 and IAA17) and three ARF transcriptional regulators (ARF6, ARF8
567 and ARF17), which control AR initiation by modulating JA homeostasis, controlling either
568 the conjugation through the *GH3* genes or the biosynthesis through a pathway still to be
569 identified (Figure 7 C and D).

570

571 MATERIALS AND METHODS

572

573 Plant material and growth conditions

574 The single mutants *tir1-1*, *afb1-3*, *afb2-3*, *afb3-4*, *afb4-8* and *afb5-5*, multiple mutants *tir1-*
575 *1afb2-3*, *afb2-3afb3-4*, *afb4-8afb5-5*, *tir1-1afb1-3afb3-4* and, translational fusion lines *tir1-*
576 *1pTIR1:cTIR1:GUS*, *afb2-3pAFB2:cAFB2:GUS*, *afb1-3pAFB1:cAFB2:GUS* and *afb3-*
577 *4pAFB3:cAFB3:GUS* were described in (Parry et al., 2009). Seeds of the mutants and
578 transgenic lines including those expressing *pAFB4:cAFB4:GUS* and *pAFB5:cAFB5:GUS*
579 were provided by Prof. Mark Estelle (UCSD, San Diego, CA, USA). The *iaa* T-DNA
580 insertion mutants used in this study are listed in Supplemental Table 1. All the mutants were
581 provided by the Nottingham Arabidopsis Stock Centre, except *iaa3/shy2-24*, which was
582 provided by Prof. Jason Reed (UNC, Chapel Hill, NC, USA). The mutant lines *iaa4-1*, *iaa5-*
583 *1*, *iaa6-1*, *iaa8-1*, *iaa9-1*, *iaa11-1*, *iaa12-1*, *iaa14-1*, *iaa17-6* and *iaa33-1* were previously
584 described in (Overvoorde et al., 2005). The *Arabidopsis thaliana* ecotype Columbia-0 (Col-0)
585 was used as the wild type and background for all the mutants and transgenic lines, except
586 *iaa3/shy2-24*, which had a Landsberg *erecta* (*Ler*) background. Growth conditions and
587 adventitious rooting experiments were performed as previously described (Gutierrez et al.,
588 2009; Sorin et al., 2005).

589

590 Hormone profiling experiment

591 Hypocotyls from the wild type Col-0, single mutants *tir1-1* and *afb2-3* and double mutant
592 *tir1-1afb2-3* were collected from seedlings grown as described in (Gutierrez et al., 2012).
593 Samples were prepared from six biological replicates; for each, at least 2 technical replicates
594 were used. Endogenous levels of free IAA, SA and JA as well as the conjugated form of JA,
595 JA-Ile, were determined in 20 mg of hypocotyls according to the method described in
596 (Flokova et al., 2014). The phytohormones were extracted using an aqueous solution of
597 methanol (10% MeOH/H₂O, v/v). To validate the LC-MS method, a cocktail of stable
598 isotope-labeled standards was added with the following composition: 5 pmol of [¹³C₆]IAA, 10
599 pmol of [²H₆]JA, [²H₂]JA-Ile and 20 pmol of [²H₄]SA (all from Olchemim Ltd, Czech
600 Republic) per sample. The extracts were purified using Oasis HLB columns (30 mg/1 ml,
601 Waters, Milford, MA, USA) and targeted analytes were eluted using 80% MeOH. Eluent
602 containing neutral and acidic compounds was gently evaporated to dryness under a stream of
603 nitrogen. Separation was performed on an Acquity UPLC® System (Waters, Milford, MA,
604 USA) equipped with an Acquity UPLC BEH C18 column (100 x 2.1 mm, 1.7 µm; Waters,

605 Milford, MA, USA), and the effluent was introduced into the electrospray ion source of a
606 triple quadrupole mass spectrometer Xevo™ TQ-S MS (Waters, Milford, MA, USA).

607

608 **RNA isolation and cDNA Synthesis**

609 RNAs from the hypocotyls of Col-0 and the mutants were prepared as described by (Gutierrez
610 et al., 2009; Gutierrez et al., 2012). The resulting RNA preparations were treated with DNaseI
611 using a DNAfree Kit (ThermoFisher Scientific AM1906; <https://www.thermofisher.com>) and
612 cDNA was synthesized by reverse transcribing 2 µg of total RNA using SuperScript III
613 reverse transcriptase (ThermoFisher Scientific 18064-014; <https://www.thermofisher.com>)
614 with 500 ng of oligo(dT)18 primer according to the manufacturer's instructions. The reaction
615 was stopped by incubation at 70°C for 10 min, and then the reaction mixture was treated with
616 RNaseH (ThermoFisher Scientific EN0201; <https://www.thermofisher.com>) according to the
617 manufacturer's instructions. All cDNA samples were tested by PCR using specific primers
618 flanking an intron sequence to confirm the absence of genomic DNA contamination.

619

620 **Quantitative RT-PCR experiments**

621 Transcript levels were assessed in three independent biological replicates by real-time qRT-
622 PCR), in assays with triplicate reaction mixtures (final volume 20 µl) containing 5 µl of
623 cDNA, 0.5 µM of both forward and reverse primers and 1 X FastStart SYBR Green Master
624 mix (Roche Ref: 04887352001; <https://lifescience.roche.com>). Steady state levels of
625 transcripts were quantified using primers listed in Supplemental Table 2. *APT1* and *TIP41*
626 had previously been validated as the most stably expressed genes among 11 tested in our
627 experimental procedures and were used to normalize the qRT-PCR data (Gutierrez et al.,
628 2009). The normalized expression patterns obtained using the reference genes were similar.
629 Therefore, only data normalized with *TIP41* are shown. The CT (crossing threshold value)
630 and PCR efficiency (*E*) values were used to calculate expression using the formula $E_T (CT_{WT} - CT_M) / E_R (CT_{WT} - CT_M)$, where T is the target gene, R is the reference gene, M refers to cDNA
631 from the mutant line and WT refers to cDNA from the wild type. Data for the mutants were
632 presented relative to those of the wild type, the calibrator.

634

635 **Heatmap of AUXIAA gene expression**

636 *AUXIAA* gene expression values were obtained as described previously in different organs
637 (cotyledons, hypocotyls and roots). The *AUXIAA* expression values for hypocotyls and roots

638 were calculated relative to those of the cotyledon samples as calibrator and set as 1. These
639 values were subsequently used to build a cluster heatmap using Genesis software
640 (<http://www.mybiosoftware.com/genesis-1-7-6-cluster-analysis-microarray-data.html>)(Sturn
641 et al., 2002). Genes with similar expression levels between organs were clustered based on
642 Pearson's correlation. Correlation values near 1 indicated a strong positive correlation
643 between two genes.

644

645 **Tagged protein constructs**

646 Epitope-tagged versions of ARF6, ARF8, ARF17, IAA5, IAA6, IAA7, IAA8, IAA9 and
647 IAA17 proteins were produced in pRT104-3xHA and pRT104-3xMyc plasmids (Fulop et al.,
648 2005). All plasmids displayed a 35S promoter sequence upstream of the multi-cloning site.
649 The open reading frames of *ARF6*, *ARF8*, *ARF17*, *IAA5*, *IAA6*, *IAA7*, *IAA8*, *IAA9* and *IAA17*
650 were amplified from cDNA from 7-day-old *Arabidopsis* seedlings using Finnzyme's Phusion
651 high-fidelity DNA polymerase (ThermoFisher SCIENTIFIC, F530S) protocol with gene-
652 specific primers listed in *SI Appendix* Table S3.

653 For the bimolecular functional complementation assay (BiFC), the open reading frames of
654 *ARF6*, *ARF8*, *IAA6*, *IAA9* and *IAA17* were amplified with gene-specific primers carrying
655 BgIII or KpnI restriction sites to facilitate subsequent cloning (*SI Appendix* Table S4). The
656 products obtained after PCR were digested with BgIII and KpnI prior to ligation into pSAT-
657 nEYFP and pSAT-cEYFP plasmids (Citovsky et al., 2006) that had previously been cut open
658 with the same enzymes. All constructs were verified by sequencing.

659

660 **Protoplast production and transformation**

661 Protoplasts from *Arabidopsis* cell culture or 14-day-old *Arabidopsis* seedlings were prepared
662 and transfected as previously described (Meskiene et al., 2003; Zhai et al., 2009). For CoIP,
663 10⁵ protoplasts from the *Arabidopsis* cell culture were transfected with 5 to 7.5 µg of each
664 construct.

665 For BiFC assays, *Arabidopsis* mesophyll protoplasts were co-transfected with 10 µg of each
666 construct. The protoplasts were imaged by confocal laser scanning microscopy after 24 hours
667 of incubation in the dark at room temperature.

668

669 **Co-immunoprecipitation**

670 For testing protein interactions, co-transfected protoplasts were extracted in lysis buffer
671 containing 25 mM Tris-HCl, pH 7.8, 10 mM MgCl₂, 75 mM NaCl, 5 mM EGTA, 60 mM β-

672 glycerophosphate, 1 mM dithiothreitol, 10% glycerol, 0.2% Igepal CA-630 and Protein
673 Inhibitor Cocktail (Sigma-Aldrich P9599-5ML; <http://www.sigmaaldrich.com/>). The cell
674 suspension was frozen in liquid nitrogen and then thawed on ice and centrifuged for 5 min at
675 150 g. The resulting supernatant was mixed with 1.5 µl of anti-Myc antibody (9E10,
676 Covance; <http://www.covance.com/>) or 2 µl of anti-HA antibody (16B12, Covance;
677 <http://www.covance.com/>) for 2 h at 4°C on a rotating wheel. Immunocomplexes were
678 captured on 10 µl of Protein G-Sepharose beads (GE Healthcare, 17-0618-01), washed three
679 times in 25 mM sodium phosphate, 5% glycerol and 0.2% Igepal CA-630 buffer and then
680 eluted by boiling with 40 µl of SDS sample buffer. The presence of immunocomplexes was
681 assessed by probing protein gel blots with either anti-HA (3F10, Sigma/Roche;
682 <http://www.sigmaaldrich.com/>) or anti-Myc antibody (9E10, Covance;
683 <http://www.covance.com/>) at 1:2000 dilution.

684

685 **Cycloheximide or proteasome inhibitor treatment of transfected protoplasts**

686 Sixteen hours after protoplast transfection, cycloheximide (CHX) (SigmaAldrich C7698-1G;
687 <http://www.sigmaaldrich.com/>) was added to a final concentration of 200 µg/ml in the
688 protoplast growth medium and the protoplasts were incubated for 0, 0.5, 1, 1.5 and 2 h.
689 Afterwards, the protoplasts were harvested and the proteins extracted and analyzed by SDS-
690 PAGE and western blotting.

691 The proteasome inhibitor MG132 (SigmaAldrich M7449, http://www.sigmaaldrich.com) was
692 applied at a concentration of 50 µM 16 h after protoplasts transfection. After 2 h incubation,
693 the protoplasts were harvested, and the proteins were extracted and analyzed by SDS-PAGE
694 and western blotting. The plasmid expressing *HA₃-ARF1* was described in (Salmon et al.,
695 2008) and kindly provided by Prof. Judy Callis (UC, Davis, CA, USA).

696

697 **Proteasome inhibition in planta**

698 Seeds from Arabidopsis lines expressing HA₃:ARF1, cMyc₃:ARF6, cMyc₃:ARF8 and
699 cMyc₃:ARF17 were sterilized and sown *in vitro* as previously described (Sorin et al., 2005).
700 Plates were incubated at 4°C for 48 h for stratification and transferred to the light for 16 h at a
701 temperature of 20°C to induce germination. The plates were then wrapped in aluminum foil
702 and kept until the hypocotyl of the seedlings reached on average 6 mm. The plates were then
703 transferred back to the light for 6 days. On day 6, the seedlings were transferred to liquid
704 growth medium (GM). On day 7, the GM was removed and fresh GM without (DMSO

705 control) or with MG132 (SigmaAldrich M7449, <http://www.sigmaaldrich.com/>) at a final
706 concentration of 100 μ M was added, and the seedlings incubated for a further 2 h. After
707 incubation, the GM liquid culture was removed, and proteins were extracted and analyzed by
708 SDS-PAGE and western blotting. The Arabidopsis line expressing *HA₃-ARF1* was described
709 in (Salmon et al., 2008) and kindly provided by Prof. Judy Callis (UC, Davis, CA, USA).

710

711 **Analysis of promoter activity**

712 A 1-kb-long fragment upstream from the start codon of *IAA6*, *IAA9* and *IAA17* was amplified
713 by applying PCR to Col-0 genomic DNA. The primer sequences used are listed in *SI*
714 *Appendix* Table S5. The amplified fragments were cloned using a pENTR/D-TOPO cloning
715 kit (ThermoFisher Scientific K240020; <https://www.thermofisher.com>) and transferred into
716 the pKGWFS7 binary vector (Karimi et al., 2002) using a Gateway LR Clonase enzyme mix
717 (ThermoFisher Scientific 11791020; <https://www.thermofisher.com>) according to the
718 manufacturer's instructions. Transgenic Arabidopsis plants expressing the *promIAA6:GUS*,
719 *promIAA9:GUS* and *promIAA17:GUS* fusion were generated by *Agrobacterium tumefaciens*
720 mediated floral dipping and the expression pattern was checked in the T2 progeny of several
721 independent transgenic lines. Histochemical assays of GUS expression were performed as
722 previously described (Sorin et al., 2005).

723

724 **Confocal laser scanning microscopy**

725

726 For the BIFC assay, images of fluorescent protoplasts were obtained with a Leica TCS-SP2-
727 AOBS spectral confocal laser scanning microscope equipped with a Leica HC PL APO x 20
728 water immersion objective. YFP and chloroplasts were excited with the 488 nm line of an
729 argon laser (laser power 35%). Fluorescence emission was detected over the range 495 to 595
730 nm for the YFP construct and 670 to 730 nm for chloroplast autofluorescence. Images were
731 recorded and processed using LCS software version 2.5 (Leica Microsystems). Images were
732 cropped using Adobe Photoshop CS2 and assembled using Adobe Illustrator CS2 software
733 (Abode, <http://www.abode.com>).

734

735 **ACKNOWLEDGMENTS**

736 The authors would like to thank Prof. Mark Estelle (UCSD, San Diego, CA, USA) and Prof
737 Jason Reed (UNC, Chapel Hill, NC, USA) for providing seeds of single and multiple mutants.
738 The authors also thank Prof. Judy Callis (UC, Davis, CA, USA) for providing Arabidopsis

739 line and the plasmid expressing *HA₃-ARF1*. We also thank Hana Martinková for help with
740 phytohormone analyses. This work was supported by the Swedish Research Council (VR),
741 the Swedish Research Council for Research and Innovation for Sustainable Growth
742 (VINNOVA), the K. & A. Wallenberg Foundation, the Carl Trygger Foundation, the Carl
743 Kempe Foundation to C. B., the University of Picardie Jules Verne, the Regional Council of
744 Picardie to L.G., the European Regional Development Fund, and the Ministry of Education,
745 Youth and Sports of the Czech Republic (European Regional Development Fund-Project
746 “Plants as a tool for sustainable global development” no.
747 CZ.02.1.01/0.0/0.0/16_019/0000827) to O.N..

748

749 **ATHORS CONTRIBUTION**

750 Methodology, A.L., C.B., E.C. and S.C.; Investigation, A.L., S.C., E.C., R.L.H., Z.R., O.N.,
751 F.J., D.I.P., I.P., A.R., L.G., L.B.; Writing-original draft, A.L., S.C. and C.B; Writing-Review
752 & Editing, A.L., C.B., E.C., L.G., R.L.H., L.B., O.N.; Conceptualization C.B.; Supervision
753 C.B.; Funding Acquisition, C.B., L.G. and O.N.

754

755 **REFERENCES**

756

757 **Arase, F., Nishitani, H., Egusa, M., Nishimoto, N., Sakurai, S., Sakamoto, N., and**
758 **Kaminaka, H.** (2012). IAA8 involved in lateral root formation interacts with the TIR1
759 auxin receptor and ARF transcription factors in Arabidopsis. *PLoS One* **7**:e43414.

760 **Bellini, C., Pacurar, D.I., and Perrone, I.** (2014). Adventitious roots and lateral roots:
761 similarities and differences. *Annu. Rev. Plant Biol.* **65**:639-666.

762 **Boer, D.R., Freire-Rios, A., van den Berg, W.A., Saaki, T., Manfield, I.W., Kepinski, S.,**
763 **Lopez-Vidrieo, I., Franco-Zorrilla, J.M., de Vries, S.C., Solano, R., et al.** (2014).
764 Structural basis for DNA binding specificity by the auxin-dependent ARF transcription
765 factors. *Cell* **156**:577-589.

766 **Calderon Villalobos, L.I., Lee, S., De Oliveira, C., Ivetac, A., Brandt, W., Armitage, L.,**
767 **Sheard, L.B., Tan, X., Parry, G., Mao, H., et al.** (2012). A combinatorial TIR1/AFB-
768 Aux/IAA co-receptor system for differential sensing of auxin. *Nat. Chem. Biol.* **8**:477-
769 485.

770 **Cecchetti, V., Altamura, M.M., Brunetti, P., Petrocelli, V., Falasca, G., Ljung, K.,**
771 **Costantino, P., and Cardarelli, M.** (2013). Auxin controls Arabidopsis anther
772 dehiscence by regulating endothecium lignification and jasmonic acid biosynthesis.
773 *Plant J.* **74**:411-422.

774 **Chapman, E.J., and Estelle, M.** (2009). Mechanism of auxin-regulated gene expression in
775 plants. *Annu. Rev. Genet.* **43**:265-285.

776 **Citovsky, V., Lee, L.Y., Vyas, S., Glick, E., Chen, M.H., Vainstein, A., Gafni, Y., Gelvin,**
777 **S.B., and Tzfira, T.** (2006). Subcellular localization of interacting proteins by
778 bimolecular fluorescence complementation in planta. *J. Mol. Biol.* **362**:1120-1131.

779 **De Rybel, B., Vassileva, V., Parizot, B., Demeulenaere, M., Grunewald, W., Audenaert,**
780 **D., Van Campenhout, J., Overvoorde, P., Jansen, L., Vanneste, S., et al.** (2010). A
781 novel aux/IAA28 signaling cascade activates GATA23-dependent specification of
782 lateral root founder cell identity. *Curr. Biol.* **20**:1697-1706.

783 **De Smet, I., Lau, S., Voss, U., Vanneste, S., Benjamins, R., Rademacher, E.H., Schlereth,**
784 **A., De Rybel, B., Vassileva, V., Grunewald, W., et al.** (2010). Bimodular auxin
785 response controls organogenesis in Arabidopsis. *Proc. Natl. Acad. Sci. U S A* **107**:2705-
786 2710.

787 **Dello Ioio, R., Nakamura, K., Moubayidin, L., Perilli, S., Taniguchi, M., Morita, M.T.,**
788 **Aoyama, T., Costantino, P., and Sabatini, S.** (2008). A genetic framework for the
789 control of cell division and differentiation in the root meristem. *Science* **322**:1380-1384.

790 **Dharmasiri, N., Dharmasiri, S., and Estelle, M.** (2005a). The F-box protein TIR1 is an
791 auxin receptor. *Nature* **435**:441-445.

792 **Dharmasiri, N., Dharmasiri, S., Weijers, D., Lechner, E., Yamada, M., Hobbie, L.,**
793 **Ehrismann, J.S., Jurgens, G., and Estelle, M.** (2005b). Plant development is
794 regulated by a family of auxin receptor F box proteins. *Dev. Cell.* **9**:109-119.

795 **Flokova, K., Tarkowska, D., Miersch, O., Strnad, M., Wasternack, C., and Novak, O.**
796 (2014). UHPLC-MS/MS based target profiling of stress-induced phytohormones.
797 *Phytochemistry* **105**:147-157.

798 **Fukaki, H., Tameda, S., Masuda, H., and Tasaka, M.** (2002). Lateral root formation is
799 blocked by a gain-of-function mutation in the SOLITARY-ROOT/IAA14 gene of
800 *Arabidopsis*. *Plant J.* **29**:153-168.

801 **Fulop, K., Pettko-Szandtner, A., Magyar, Z., Miskolczi, P., Kondorosi, E., Dudits, D.,**
802 **and Bako, L.** (2005). The Medicago CDKC;1-CYCLINT;1 kinase complex
803 phosphorylates the carboxy-terminal domain of RNA polymerase II and promotes
804 transcription. *Plant J.* **42**:810-820.

805 **Geiss, G., Gutierrez, L., and Bellini, C.** (2009). Adventitious root formation: new insights
806 and perspective. In: *Root Development - Annual Plant Reviews --Beeckman, T., ed.*
807 London: A John Wiley & Sons, Ltd. 127-156.

808 **Gray, W.M., Kepinski, S., Rouse, D., Leyser, O., and Estelle, M.** (2001). Auxin regulates
809 SCF(TIR1)-dependent degradation of AUX/IAA proteins. *Nature* **414**:271-276.

810 **Guilfoyle, T.J., and Hagen, G.** (2007). Auxin response factors. *Curr. Opin. Plant Biol.*
811 **10**:453-460.

812 **Guilfoyle, T.J., and Hagen, G.** (2012). Getting a grasp on domain III/IV responsible for
813 Auxin Response Factor-IAA protein interactions. *Plant Sci.* **190**:82-88.

814 **Gutierrez, L., Bussell, J.D., Pacurar, D.I., Schwambach, J., Pacurar, M., and Bellini, C.**
815 (2009). Phenotypic plasticity of adventitious rooting in *Arabidopsis* is controlled by
816 complex regulation of AUXIN RESPONSE FACTOR transcripts and microRNA
817 abundance. *Plant Cell* **21**:3119-3132.

818 **Gutierrez, L., Mongelard, G., Flokova, K., Pacurar, D.I., Novak, O., Staswick, P.,**
819 **Kowalczyk, M., Pacurar, M., Demailly, H., Geiss, G., et al.** (2012). Auxin controls

820 Arabidopsis adventitious root initiation by regulating jasmonic acid homeostasis. *Plant*
821 *Cell* **24**:2515-2527.

822 **Hamann, T., Benkova, E., Baurle, I., Kientz, M., and Jurgens, G.** (2002). The Arabidopsis
823 BODENLOS gene encodes an auxin response protein inhibiting MONOPTEROS-
824 mediated embryo patterning. *Genes Dev.* **16**:1610-1615.

825 **Havens, K.A., Guseman, J.M., Jang, S.S., Pierre-Jerome, E., Bolten, N., Klavins, E. and**
826 **Nemhauser, J.** (2012) A Synthetic Approach Reveals Extensive Tunability of Auxin
827 Signaling. *Plant Phys.* **160**: 135-142

828 **Karimi, M., Inze, D., and Depicker, A.** (2002). GATEWAY vectors for Agrobacterium-
829 mediated plant transformation. *Trends Plant Sci.* **7**:193-195.

830 **Kepinski, S., and Leyser, O.** (2005). The Arabidopsis F-box protein TIR1 is an auxin
831 receptor. *Nature* **435**:446-451.

832 **Korasick, D.A., Westfall, C.S., Lee, S.G., Nanao, M.H., Dumas, R., Hagen, G., Guilfoyle,**
833 **T.J., Jez, J.M., and Strader, L.C.** (2014). Molecular basis for AUXIN RESPONSE
834 FACTOR protein interaction and the control of auxin response repression. *Proc. Natl.*
835 *Acad. Sci. U S A* **111**:5427-5432.

836 **Lakehal, A., and Bellini, C.** (2019). Control of adventitious root formation: insights into
837 synergistic and antagonistic hormonal interactions. *Physiol Plant.* **165**:90-100.

838 **Lavenus, J., Goh, T., Roberts, I., Guyomarc'h, S., Lucas, M., De Smet, I., Fukaki, H.,**
839 **Beeckman, T., Bennett, M., and Laplaze, L.** (2013). Lateral root development in
840 Arabidopsis: fifty shades of auxin. *Trends Plant Sci.* **18**:450-458.

841 **Magyar, Z., De Veylder, L., Atanassova, A., Bako, L., Inze, D., and Bogre, L.** (2005). The
842 role of the Arabidopsis E2FB transcription factor in regulating auxin-dependent cell
843 division. *Plant Cell* **17**:2527-2541.

844 **Meskiene, I., Baudouin, E., Schweighofer, A., Liwosz, A., Jonak, C., Rodriguez, P.L.,**
845 **Jelinek, H., and Hirt, H.** (2003). Stress-induced protein phosphatase 2C is a negative
846 regulator of a mitogen-activated protein kinase. *J. Biol. Chem.* **278**:18945-18952.

847 **Nagpal, P., Ellis, C.M., Weber, H., Ploense, S.E., Barkawi, L.S., Guilfoyle, T.J., Hagen,**
848 **G., Alonso, J.M., Cohen, J.D., Farmer, E.E., et al.** (2005). Auxin response factors
849 ARF6 and ARF8 promote jasmonic acid production and flower maturation.
850 *Development* **132**:4107-4118.

851 **Nanao, M.H., Vinos-Poyo, T., Brunoud, G., Thevenon, E., Mazzoleni, M., Mast, D.,**
852 **Laine, S., Wang, S., Hagen, G., Li, H., et al.** (2014). Structural basis for
853 oligomerization of auxin transcriptional regulators. *Nat. Commun.* **5**:3617.

854 **Okushima, Y., Overvoorde, P. J., Arima, K., Alonso, J. M., Chan, A., Chang, C., Ecker,**
855 **J. R., Hughes, B., Lui, A., et al. (2005).** Functional genomic analysis of the AUXIN
856 RESPONSE FACTOR gene family members in *Arabidopsis thaliana*: unique and
857 overlapping functions of ARF7 and ARF19. *Plant Cell* **17**: 444-463

858 **Orosa-Puente, B., Leftley, N., von Wangenheim, D., Banda, J., Srivastava, A.K., Hill, K.,**
859 **Truskina, J., Bhosale, R., Morris, E., Srivastava, M., et al. (2018).** Root branching
860 toward water involves posttranslational modification of transcription factor ARF7.
861 *Science* **362**:1407-1410.

862 **Overvoorde, P.J., Okushima, Y., Alonso, J.M., Chan, A., Chang, C., Ecker, J.R.,**
863 **Hughes, B., Liu, A., Onodera, C., Quach, H., et al. (2005).** Functional genomic
864 analysis of the AUXIN/INDOLE-3-ACETIC ACID gene family members in
865 *Arabidopsis thaliana*. *Plant Cell* **17**:3282-3300.

866 **Pacurar, D.I., Pacurar, M.L., Bussell, J.D., Schwambach, J., Pop, T.I., Kowalczyk, M.,**
867 **Gutierrez, L., Cavel, E., Chaabouni, S., Ljung, K., et al. (2014a).** Identification of
868 new adventitious rooting mutants amongst suppressors of the *Arabidopsis thaliana*
869 *superroot2* mutation. *J Exp Bot* **65**:1605-1618.

870 **Pacurar, D.I., Perrone, I., and Bellini, C. (2014b).** Auxin is a central player in the hormone
871 cross-talks that control adventitious rooting. *Physiol. Plant.* **151**:83-96.

872 **Parcy, F., Vernoux, T., and Dumas, R. (2016).** A Glimpse beyond Structures in Auxin-
873 Dependent Transcription. *Trends Plant Sci.* **21**:574-583.

874 **Parry, G., Calderon-Villalobos, L.I., Prigge, M., Peret, B., Dharmasiri, S., Itoh, H.,**
875 **Lechner, E., Gray, W.M., Bennett, M., and Estelle, M. (2009).** Complex regulation
876 of the TIR1/AFB family of auxin receptors. *Proc. Natl. Acad. Sci. U S A* **106**:22540-
877 22545.

878 **Ramos, J.A., Zenser, N., Leyser, O., and Callis, J. (2001).** Rapid degradation of
879 auxin/indoleacetic acid proteins requires conserved amino acids of domain II and is
880 proteasome dependent. *Plant Cell* **13**:2349-2360.

881 **Salmon, J., Ramos, J., and Callis, J. (2008).** Degradation of the auxin response factor
882 ARF1. *Plant J.* **54**:118-128.

883 **Shani, E., Salehin, M., Zhang, Y., Sanchez, S.E., Doherty, C., Wang, R., Mangado, C.C.,**
884 **Song, L., Tal, I., Pisanty, O., et al. (2017).** Plant Stress Tolerance Requires Auxin-
885 Sensitive Aux/IAA Transcriptional Repressors. *Curr. Biol.* **27**:437-444.

886 **Sheng, L., Hu, X., Du, Y., Zhang, G., Huang, H., Scheres, B., and Xu, L.** (2017). Non-
887 canonical WOX11-mediated root branching contributes to plasticity in Arabidopsis root
888 system architecture. *Development* **144**:3126-3133.

889 **Sorin, C., Bussell, J.D., Camus, I., Ljung, K., Kowalczyk, M., Geiss, G., McKhann, H.,**
890 **Garcion, C., Vaucheret, H., Sandberg, G., et al.** (2005). Auxin and light control of
891 adventitious rooting in Arabidopsis require ARGONAUTE1. *Plant Cell* **17**:1343-1359.

892 **Sorin, C., Negroni, L., Balliau, T., Corti, H., Jacquemot, M.P., Davanture, M.,**
893 **Sandberg, G., Zivy, M., and Bellini, C.** (2006). Proteomic analysis of different mutant
894 genotypes of Arabidopsis led to the identification of 11 proteins correlating with
895 adventitious root development. *Plant Physiol* **140**:349-364.

896 **Staswick, P.E., Serban, B., Rowe, M., Tiryaki, I., Maldonado, M.T., Maldonado, M.C.,**
897 **and Suza, W.** (2005) Characterization of an Arabidopsis enzyme family that conjugates
898 amino acids to indole-3-acetic acid. *Plant Cell* **17**: 616–627

899 **Steffens, B., and Rasmussen, A.** (2016). The Physiology of Adventitious Roots. *Plant*
900 *Physiol* **170**:603-617.

901 **Sturn, A., Quackenbush, J., and Trajanoski, Z.** (2002). Genesis: cluster analysis of
902 microarray data. *Bioinformatics* **18**:207-208.

903 **Sun, J., Qi, L., Li, Y., Zhai, Q., and Li, C.** (2013). PIF4 and PIF5 transcription factors link
904 blue light and auxin to regulate the phototropic response in Arabidopsis. *Plant Cell*
905 **25**:2102-2114.

906 **Szemenyei, H., Hannon, M., and Long, J.A.** (2008). TOPLESS mediates auxin-dependent
907 transcriptional repression during Arabidopsis embryogenesis. *Science* **319**:1384-1386.

908 **Takato, S., Kakei, Y., Mitsui, M., Ishida, Y., Suzuki, M., Yamazaki, C., Hayashi, K. I.,**
909 **Ishii, T., Nakamura, A., Soeno, K., and Shimada, Y.** (2017) Auxin signaling through
910 SCF(TIR1/AFBs) mediates feedback regulation of IAA biosynthesis. *Biosci.*
911 *Biotechnol. Biochem.* **81**: 320-1326

912 **Tan, X., Calderon-Villalobos, L.I., Sharon, M., Zheng, C., Robinson, C.V., Estelle, M.,**
913 **and Zheng, N.** (2007). Mechanism of auxin perception by the TIR1 ubiquitin ligase.
914 *Nature* **446**:640-645.

915 **Tatematsu, K., Kumagai, S., Muto, H., Sato, A., Watahiki, M.K., Harper, R.M., Liscum,**
916 **E., and Yamamoto, K.T.** (2004). MASSUGU2 encodes Aux/IAA19, an auxin-
917 regulated protein that functions together with the transcriptional activator NPH4/ARF7
918 to regulate differential growth responses of hypocotyl and formation of lateral roots in
919 Arabidopsis thaliana. *Plant Cell* **16**:379-393.

920 **Vernoux, T., Brunoud, G., Farcot, E., Morin, V., Van den Daele, H., Legrand, J., Oliva,**
921 **M., Das, P., Larrieu, A., Wells, D., et al.** (2011). The auxin signalling network
922 translates dynamic input into robust patterning at the shoot apex. *Mol. Syst. Biol.* **7**:508.
923 **Wang, H., Jones, B., Li, Z., Frasse, P., Delalande, C., Regad, F., Chaabouni, S., Latche,**
924 **A., Pech, J.C., and Bouzayen, M.** (2005). The tomato Aux/IAA transcription factor
925 IAA9 is involved in fruit development and leaf morphogenesis. *Plant Cell* **17**:2676-
926 2692.
927 **Wang, R., and Estelle, M.** (2014). Diversity and specificity: auxin perception and signaling
928 through the TIR1/AFB pathway. *Curr. Opin. Plant Biol.* **21**:51-58.
929 **Wasternack, C. and Feussner, I.** (2017) The Oxylin Pathways: Biochemistry and
930 Function. *Annu. Rev. Plant Biol.* **69**:363-386
931 **Weijers, D., Sauer, M., Meurette, O., Friml, J., Ljung, K., Sandberg, G., Hooykaas, P.,**
932 **and Offringa, R.** (2005). Maintenance of embryonic auxin distribution for apical-basal
933 patterning by PIN-FORMED-dependent auxin transport in Arabidopsis. *Plant Cell*
934 **17**:2517-2526.
935 **Weijers, D., and Wagner, D.** (2016). Transcriptional Responses to the Auxin Hormone.
936 *Annu. Rev. Plant Biol.* **67**:539-574.
937 **Xuan, W., Audenaert, D., Parizot, B., Moller, B. K., Njo, M. F., De Rybel, B., De Rop,**
938 **G., Van Isterdael, G., Mahonen, A. P et al.** (2015) Root Cap-Derived Auxin Pre-
939 patterns the Longitudinal Axis of the Arabidopsis Root. *Curr. Biol.* **25**:1381-1388
940 **Zhai, Z., Jung, H.I., and Vatamaniuk, O.K.** (2009). Isolation of protoplasts from tissues of
941 14-day-old seedlings of Arabidopsis thaliana. *J. Vis. Exp.* **30**:1149
942 **Zhao, Z., Zhang, Y., Liu, X., Zhang, X., Liu, S., Yu, X., Ren, Y., Zheng, X., Zhou, K.,**
943 **Jiang, L. et al.** (2013) A role for a dioxygenase in auxin metabolism and reproductive
944 development in rice. *Dev. Cell* **27**:113-122
945

946 **FIGURE LEGENDS**

947

948 **Figure 1: TIR1 and AFB2 control adventitious root initiation by modulating *GH3.3*,**
949 ***GH3.5* and *GH3.6* expression**

950 (A) Average numbers of adventitious roots in *tir/afb* mutants. Seedlings were first etiolated in
951 the dark until their hypocotyls were 6 mm long and then transferred to the light for 7 days.
952 Data were obtained from 3 biological replicates; for each, data for at least 30 seedlings were
953 pooled and averaged. Errors bars indicate \pm SE. A non-parametric Kruskal-Wallis test
954 followed by the Dunn's multiple comparison post-test indicated that only mutations in the
955 *TIR1* and *AFB2* genes significantly affected the initiation of adventitious roots ($n > 30$; $P <$
956 0.001).

957 (B) Expression pattern of TIR1 and AFB2 proteins. GUS staining of *tir1-1pTIR1:cTIR1-GUS*
958 and *afb2-3AFB2:cAFB2-GUS* translational fusions (arranged from left to right in each panel)
959 in seedlings grown in the dark until their hypocotyls were 6 mm long (T0) and 9 h (T9) and
960 72 h (T72) after their transfer to the light. (a) and (b) Close-ups from hypocotyl regions
961 shown for T72. Scale bar = 2 mm

962 (C) Quantification by qRT-PCR of *GH3.3*, *GH3.5* and *GH3.6* transcripts in hypocotyls of
963 *tir1-1* and *afb2-3* single mutants and the *tir1-1afb2-3* double mutant. mRNAs were extracted
964 from hypocotyls of seedlings grown in the dark until the hypocotyl reached 6 mm (T0) and
965 after their transfer to the light for 9 h or 72 h. The gene expression values are relative to the
966 expression in the wild type, for which the value was set to 1. The scale is a log₁₀ scale, the
967 extremum and minimum of each graph have been optimized according to the expression
968 values. Error bars indicate \pm SE obtained from three independent biological replicates. One-
969 way ANOVA combined with Dunnett's multiple comparison test indicated that in some cases,
970 the relative amount of mRNA was significantly different from the wild type (denoted by *, P
971 < 0.001 ; $n = 3$).

972

973 **Figure 2: TIR1 and AFB2 control adventitious root initiation by modulating jasmonate**
974 **homeostasis**

975 (A) to (D) The endogenous contents of free IAA (D), free SA (B), free JA (C) and JA-Ile (D)
976 were quantified in the hypocotyls of wild type Col-0, single mutants *tir1-1* and *afb2-3* and
977 double mutant *tir1-1afb2-3* seedlings grown in the dark until the hypocotyl reached 6 mm
978 (T0) and after their transfer to the light for 9 h (T9) or 72 h (T72). Error bars indicate \pm SD of
979 six biological replicates. One-way ANOVA combined with Dunnett's multiple comparison
980 test indicated that in some cases, values were significantly different from those of the wild-

981 type Col-0 (denoted by *, $P < 0.05$; $n = 6$).

982

983 **Figure 3: A mutation in TIR1 induces an upregulation of the JA biosynthesis genes**

984 (A) to (C) Relative transcript amount of genes involved in JA biosynthesis (*OPCLI*, *OPR3*,
985 *LOX2*, *AOCI*, *AOC2*, *AOC3*, *AOC4*). The transcript amount was assessed by qRT-PCR using
986 mRNAs extracted from hypocotyls of seedlings grown in the dark until the hypocotyl reached
987 6 mm (T0) and after their transfer to the light for 9 h (T9) or 72 h (T72). The gene expression
988 values are relative to the expression in the wild type, for which the value was set to 1. Error
989 bars indicate \pm SE obtained from three independent biological replicates. The scale is a log10
990 scale, the extremum and minimum of each graph have been optimized according to the
991 expression values. One-way ANOVA combined with the Dunnett's multiple comparison test
992 indicated that in some cases, the relative amount of mRNA was significantly different from
993 the wild type (denoted by *, $P < 0.001$; $n = 3$).

994

995 **Figure 4: IAA6, IAA9 and IAA17 are involved in the control of adventitious root**
996 **initiation**

997

998 (A) Average numbers of ARs assessed in 15 *aux/iaa* knockout mutants. (B) Average numbers
999 of ARs in *iaa6-1*, *iaa6-2*, *iaa9-1*, *iaa9-2*, *iaa17-2*, *iaa17-3* and *iaa17-6* mutant alleles. (C)
1000 Average numbers of ARs in single *iaa6-1*, *iaa9-1* and *iaa17-6* single, double and triple
1001 mutants.

1002 (A) to (C) Seedlings were first etiolated in the dark until their hypocotyls were 6 mm long and
1003 then transferred to the light for 7 days. Data were obtained from 3 biological replicates; for
1004 each, data for at least 30 seedlings were pooled and averaged. Errors bars indicate \pm SE. In
1005 (A) and (B), one-way ANOVA combined with Dunnett's multiple comparison post-test
1006 indicated that in some cases, differences observed between the mutants and the corresponding
1007 wild type were significant (denoted by *, $P < 0.001$, $n > 30$). In (C), one-way ANOVA
1008 combined with Tukey's multiple comparison post-test indicated significant differences
1009 (denoted by different letters, $P < 0.001$, $n > 30$)

1010 (D) to (H) Expression pattern of *IAA6*, *IAA9* and *IAA17* during the initial steps of AR
1011 formation. GUS staining of *promIAA6:GUS*, *promIAA9:GUS* and *promIAA17:GUS* (arranged
1012 from left to right in each panel) in seedlings grown in the dark until their hypocotyls were 6
1013 mm long (D), after additional 48 h (E) and 72 h (G) after in the dark, and 48 h (F) and 72 h
1014 (H) after their transfer to the light. Bars = 5 mm.

1015

1016 **Figure 5: IAA6, IAA9 and IAA17 repressor proteins physically interact with ARF6**
1017 **and/or ARF8, while ARF6 interacts with itself to form a homodimer**

1018 (A) to (E) Co-immunoprecipitation (CoIP) assay. Arabidopsis protoplasts were transfected
1019 with a HA₃-tagged version of *IAA6*, *IAA9* or *IAA17* constructs and/or a c-Myc₃-tagged version
1020 of *ARF6* or *ARF8* constructs. Proteins were immunoprecipitated with anti-Myc antibodies and
1021 submitted to anti-cMyc protein (lower panel) to confirm the presence of the ARF protein and
1022 to anti-HA gel-blot analysis to reveal the IAA partner (top panel). HA₃-IAA6-cMyc-ARF6
1023 (A), HA₃-IAA6-cMyc-ARF8 (B), HA₃-IAA9-cMyc-ARF8 (C), HA₃-IAA17-cMyc-ARF6
1024 (D), HA₃-IAA17-cMyc-ARF6 (E).

1025 (F) to (H) Arabidopsis protoplasts were transfected with HA₃-tagged and c-Myc₃-tagged
1026 versions of *ARF6* and/or *ARF8*. Proteins were immunoprecipitated with anti-HA antibodies
1027 and submitted to anti-HA protein (top panel) to confirm the presence of the ARF protein and
1028 to anti-cMyc antibody to reveal the ARF6 or ARF8 partner (lower panel). Only ARF6
1029 homodimer could be detected (F).

1030 (I) to (P) Confirmation of the interaction by bimolecular fluorescence complementation
1031 experiments (BiFC). Only Arabidopsis mesophyll protoplasts with intact plasma membranes,
1032 shown with bright-field light microscopy (left photo in each panel), tested positive for the
1033 presence of yellow fluorescence, indicating protein-protein interaction due to assembly of the
1034 split YFP, shown by confocal microscopy (right photo in each panel). (I) Cotransformation of
1035 10 µg nEYFP-IAA6 and 10 µg ARF6-cEYFP into protoplasts generated yellow fluorescence
1036 (false-colored green) at the nucleus surrounded by chloroplast autofluorescence (false-colored
1037 red). Fluorescence was also observed after cotransformation of 10 µg of nEYFP-IAA6 and
1038 cEYFP-ARF8 (J); nEYFP-IAA9 and cEYFP-ARF8 (K); nEYFP-IAA17 and cEYFP-ARF6
1039 (L); nEYFP-IAA17 and cEYFP-ARF8 (M), and nEYFP-ARF6 and cEYFP-ARF6 (N). No
1040 fluorescence was detected after cotransformation of 10 µg of nEYFP-ARF6 and cEYFP-
1041 ARF8 (O) or nEYFP-ARF8 and cEYFP-ARF8 (P). Bars = 10 µm.

1042

1043 **Figure 6: ARF6, ARF8 and ARF17 are unstable proteins whose degradation is**
1044 **proteasome dependent**

1045 (A) to (D) Degradation kinetics of ARF6, ARF8 and ARF17 proteins. Top panel:
1046 representative anti-HA or anti-c-Myc western blot performed on total protein from wild-type
1047 Col-0 protoplasts transformed with 5 µg of plasmid DNA expressing HA₃- or cMyc₃- tagged
1048 proteins and mock treated with DMSO (-) or treated with 200 µg/ml of cycloheximide. Lower
1049 panel: Amido Black staining of the membrane indicating protein loading.

1050 (E) Effect of MG132 on the degradation of the tagged ARF proteins in protoplasts. Top panel:
1051 representative anti-HA western blot performed on total protein from wild-type Col-0
1052 protoplasts transformed with 5 µg of plasmid DNA expressing HA₃- or cMyc₃- ARF6, ARF8
1053 and ARF17 or 15 µg of plasmid DNA expressing HA₃-ARF1 treated with MG132 (+) or
1054 mock treated with DMSO (-) for 2 h. Lower panel: Amido Black staining of the membrane
1055 indicating protein loading.

1056 (F) Effect of MG132 on the degradation of the tagged ARF proteins *in Planta*. Top panel:
1057 representative western blot performed on total protein extracted from 7-day-old seedlings
1058 expressing HA₃-ARF1, Myc₃-ARF6, Myc₃-ARF8 or Myc₃-ARF17 treated with MG132 (+) or
1059 mock treated with DMSO (-) for 2 h. Lower panel: Amido Black staining of the membrane
1060 indicating protein loading.

1061 ImageJ (<https://imagej.nih.gov/ij/>) was used for densitometry imaging to analyze intensity of
1062 western blot bands. The ARFs staining intensities were quantified with the area of the major
1063 pic of each cMyc- or HA-tagged versions of the proteins (above 100kDa) and divided by the
1064 density of the corresponding major loading protein. Relative target protein accumulation at t0
1065 for the CHX treatment (A,B,C and D) or no MG132 (E and F) was set to 1 and then compared
1066 across all lanes, to assess changes across samples and ARFs stability.

1067

1068 **Figure 7: *TIR1/AFB2-Aux/IAA6/9/17-ARF6/8* and *ARF17* signaling module is involved**
1069 **in the control of adventitious root initiation upstream of *GH3.3*, *GH3.5* and *GH3.6***

1070 (A) Relative transcript amount of *GH3.3*, *GH3.5*, *GH3.6*, *GH3.10* and *GH3.11* genes in
1071 hypocotyls of *iaa4-1*, *iaa6-1*, *iaa9-1* and *iaa17-6* single mutants.

1072 (B) Relative transcript amount of *IAA6*, *IAA9* and *IAA17* genes in hypocotyls of *iaa4-1*, *iaa6-*
1073 *1*, *iaa9-1* and *iaa17-6* single mutants.

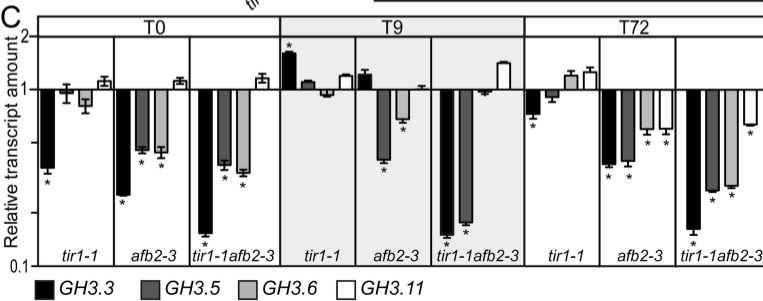
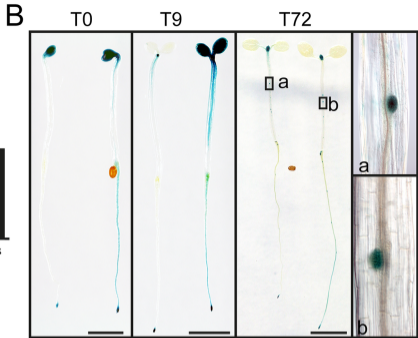
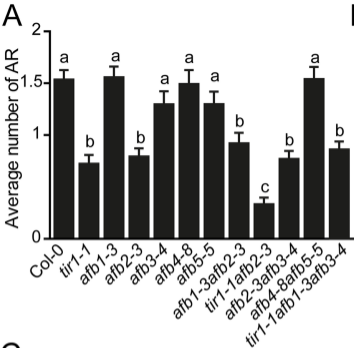
1074 In (A) and (B), mRNAs were extracted from hypocotyls of seedlings grown in the dark until
1075 the hypocotyl reached 6 mm and then transferred to the light for 72 h. Gene expression values
1076 are relative to expression in the wild type, for which the value was set to 1. The scale is a
1077 log₁₀ scale, the extremum and minimum of each graph have been optimized according to the
1078 expression values. Error bars indicate ± SE obtained from three independent biological
1079 replicates. One-way ANOVA combined with Dunnett's multiple comparison test indicated
1080 that in some cases, the relative amount of mRNA was significantly different from the wild
1081 type

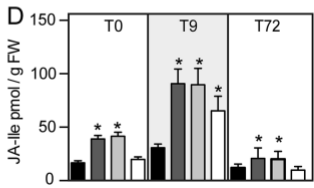
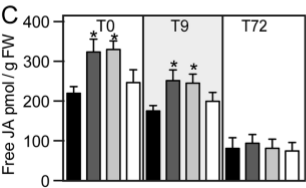
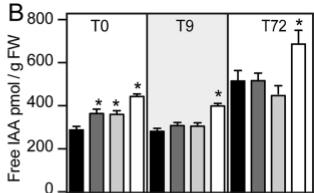
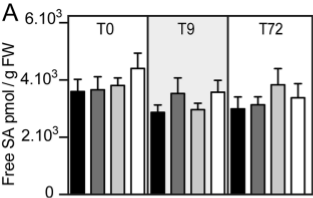
1082 (C) Adventitious root initiation is controlled by a subtle balance of ARF activators and
1083 repressor acting upstream of JA signaling (Gutierrez et al., 2012). Under steady-state

1084 conditions there is a balance between the positive regulators ARF6 and ARF8 and the
1085 negative regulator ARF17. The three ARFs are regulated at the transcriptional and post-
1086 transcriptional levels (Gutierrez et al., 2009) and their proteasome-dependent degradation
1087 possibly contributes to maintain their balance. IAA6, IAA9 and IAA17 protein repress the
1088 transcriptional activity of ARF6 and ARF8. The negative regulator ARF17 either interacts
1089 with ARF6 and/or ARF8 to inhibit their transcriptional activity or competes for the AuxRE
1090 elements in the promoters of the *GH3* genes. TIR1 protein controls JA biosynthesis through a
1091 pathway yet to be identified. (D) When the auxin content increases the Aux/IAA proteins
1092 form an auxin coreceptor complex with TIR1 and/or AFB2 and are sent for degradation
1093 through the 26S proteasome. In this case, the transcriptional activity of ARF6 and ARF8 is
1094 released. Therefore, the balance is shifted towards the positive regulators and results in the
1095 induction of *GH3* gene expression. The negative effect of TIR1 on JA biosynthesis is
1096 accentuated. The increased conjugation of JA by the three GH3 enzymes combined to the
1097 downregulation of JA biosynthesis will reduce the JA pool and subsequently downregulate JA
1098 signaling, resulting in increased AR initiation.

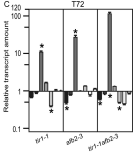
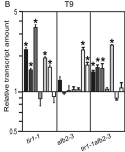
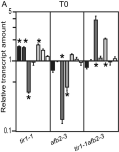
1099

1100





Col-0
 tir1-1
 afb2-3
 tir1-1afb2-3



OPCL1 OPR3 LOX2 AOC1 AOC2 AOC3 AOC4

